Comparative study of hydrogen storage and battery storage in grid connected photovoltaic system: storage sizing and rule-based operation

Yang Zhang[a, b, *], Pietro Elia Campana[c], Anders Lundblad[a, c], Jinyue Yan[a, c, *]

[a] Department of Chemical Engineering and Technology, School of Chemical Science and Engineering, KTH Royal Institute of Technology, SE-10044 Stockholm, Sweden

[b] Ningbo RX New Materials Tech. Co. Ltd., 315200 Ningbo, China

[c] School of Business, Society & Engineering, Mälardalen University, SE-72123 Västerås, Sweden

*Corresponding author: Yang Zhang & Jinyue Yan

Mail address: Teknikringen 42, SE-11428 Stockholm, Sweden

Yang Zhang: yaz@kth.se

Pietro Elia Campana: pietro.campana@mdh.se

Anders Lundblad: lundbla@kth.se

Jinyue Yan: jinyue@kth.se

Comparative study of hydrogen storage and battery storage in grid connected photovoltaic system: storage sizing and rule-based operation[1]

Yang Zhang[a, b, *], Pietro Elia Campana[c], Anders Lundblad[a, c], Jinyue Yan[a, c, *]

Abstract: The paper studies grid connected photovoltaic(PV)-hydrogen/battery systems. The storage component capacities and the rule-based operation strategy parameters are simultaneously optimized by the Genetic Algorithm. Three operation strategies for the hydrogen storage, namely conventional operation strategy, peak shaving strategy and hybrid operation strategy, are compared under two scenarios based on the pessimistic and optimistic costs. The results indicate that the hybrid operation strategy, which combines the conventional operation strategy and the peak shaving strategy, is advantageous in achieving higher Net Present Value (NPV) and Self Sufficiency Ratio (SSR). Hydrogen storage is further compared with battery storage. Under the pessimistic cost scenario, hydrogen storage results in poorer performance in both SSR and NPV. While under the optimistic cost scenario, hydrogen storage achieves higher NPV. Moreover, when taking into account the grid power fluctuation, hydrogen storage achieves better performance in all three optimization objectives, which are NPV, SSR and GI (Grid Indicator).

Keywords: Photovoltaic; Hydrogen Storage; Battery Storage; Buildings; Operation Strategy; Genetic Algorithm

[1] The short version of the paper was presented at REM2016 on April 19-21, Maldives. This paper is a substantial extension of the short version.

Nomenclature

Symbol	Unit	Description
$C_{O\&M,y}$	SEK	Operation and maintenance cost at year y
$C_{R,y}$	SEK	Replacement cost at year y
CAP_i	kW/kWh/kg	Capacity for component *i*
$El_{r,t}$	SEK/kWh	Retail electricity price at time t
$El_{w,t}$	SEK/kWh	Wholesale electricity price at time t
Inv	SEK	Investment cost
$P_{Net,t}$	kW	Net Power at time t
$P_{L,t}$	kW	Load at time t
$P_{PV,t}$	kW	PV production at time t
$P_{HS,t}$	kW	Hydrogen storage system power at time t
$P_{Batt,t}$	kW	Battery power at time t
$P_{G,t}$	kW	Grid power at time t
$P_{Gim,t}$	kW	Imported grid power at time t
$P_{Gex,t}$	kW	Exported grid power at time t
P_E	kW	Export limit
P_{PL}	kW	Grid peak limit
P_{CL}	kW	Charge limit
P_{PR}	kW	Grid peak power reduction
R_y	SEK	System revenue at year y
$R_{ER,y}$	SEK	Electricity reduction revenue at year y
$R_{EX,y}$	SEK	Export revenue at year y
$R_{PS,y}$	SEK	Peak shaving revenue at year y
$r_{O\&M,i}$	%/Year	O&M Ratio for component *i*
$SOH2_L$	%	State of hydrogen level limit
SOC_t	%	State of Charge at time *t*
t_s	h	Conventional operation start time
t_e	h	Conventional operation end time
UIC_i	SEK/Capacity Unit	Unit Investment Cost for component *i*

Abbreviations

Abbreviations	Description
DOD	Depth of Discharge
Elspot	Electricity Spot
Fit	Feed-in-tariff
GA	Genetic Algorithm
GI	Grid Indicator
NPV	Net Present Value
PV	Photovoltaic
SSR	Self Sufficiency Ratio
TOU	Time-of-Use

1 Introduction

There is a rapid increase in installed Photovoltaic (PV) capacity in recent years. 38.7GW were installed worldwide in 2014 [1]. Supporting policies, such as feed-in-tariff and net-metering, act as important incentives for the rapid increase [2]. However, with the decreasing cost of PV modules and the PV intermittency problem, the supporting incentives are expected to be gradually phased out. The PV self-consumption becomes more attractive because the self-consumed electricity generally has more economic values than the exported electricity [3, 4]. The self-consumed electricity not only generates economic benefits to the PV system owner, but also improves the power quality. Energy storage plays a vital role for increasing PV self-consumption [4]. However, increased capital investment with energy storage calls for detailed analysis and optimal solutions should be carried out to simultaneously determine the energy storage method, the storage capacity and the operation strategy.

Many studies have focused on the optimization of either storage capacity or operation strategy. Genetic Algorithm [5] and particle swarm optimization [6] were introduced to find the optimal component capacity. Dynamic programming was employed to determine the 24-hour ahead power schedule [7]. A short-term scheduling method using a Lagrangian relaxation-based optimization algorithm was suggested in Lu et al. [8]. There are also approaches aiming at achieving the optimal storage capacity and operation strategy simultaneously. Ru et al. [9] and Khalilpour et al. [10] addressed the sizing problem with consideration of the operation strategies. Zhang et al. summarized the existing methods and proposed an approach, which simultaneously obtained the storage capacity and rule-based operation strategies [11].

Battery is usually chosen as the energy storage method, because it is considered as a mature technology [12]. However, it is not suitable for long-term storage because of the low energy density and high self-discharge rate. Thus battery storage cannot address the seasonal mismatch between the PV production and load, which is quite common in residential buildings of Nordic countries. On the other hand, hydrogen storage converts electricity into the form of hydrogen. It has higher energy density and insignificant leakage (discharge) rate [13]. It is an appropriate long-term storage method to solve the seasonal mismatch problem [14], and its potential application in residential building are closely followed by research institutions and industry stakeholders [15]. Another advantage of hydrogen storage is the flexible combination of charge power, discharge power and storage capacity, because each of them is determined by separate component. The major drawbacks of hydrogen storage are the high investment cost and low round trip efficiency (around 35%) [14]. Literature survey is conducted below to explain the current research gap in the comparison between hydrogen storage and battery storage.

Some studies on the off-grid system employed both battery storage and hydrogen storage. Bigdeli suggested that fuzzy logic control and quantum behaved particle swarm optimization have better performance than other control algorithms [16]. Carapellucci et al. presented an optimization tool by using a hybrid genetic-simulated annealing algorithm. However, the optimization of operation strategies is not included [17]. Castaňeda et al. compared three control strategies for the combined battery and hydrogen storage system [18]. However, the operation strategies are all predefined and fixed.

Hydrogen storage and battery storage are also employed in grid-connected systems. Parra et al. studied the benefits of battery storage and hydrogen storage for a grid-connected single house [19]. Marino et al. carried out techno-economic analysis of a grid-connected hydrogen storage system and concluded that the system can only be realized with subsidies [20]. Avril et al. studied a grid-connected PV system with both battery storage and hydrogen storage, and carried out optimization. However, one optimization objective was to minimize the system dependency on the grid, and the operation strategy was not optimized [21]. Pellow et al. compared grid-scale hydrogen storage and battery storage. The comparison results indicated that hydrogen storage stored more electricity than battery storage through the lifetime [22]. García-Triviňo et al. carried out long-term optimization for different Energy Management Systems (EMS) and concluded that EMS can be tailored for different purposes [23].

The literature review indicates that there are few studies that simultaneously optimize the hydrogen storage capacity and the operation strategy. The comparison between hydrogen storage and battery storage, especially under the seasonal mismatch case, is also lacking. This study aims to fill the above-mentioned research gap. However, it restricts the scope to employ either hydrogen storage or battery storage within the system. The combined battery and hydrogen storage system is not considered in this study.

Based on our previous study [11], we extend the methodology through developing hydrogen storage model and introducing new operation strategies for the grid-connected PV-hydrogen storage system, building a ready-to-use tool for the system. The battery storage and hydrogen storage are further compared with the extended methodology.

The paper is organized as follows: Section 1 is the introduction; Section 2 gives the system layout and component models; Section 3 discusses about the objectives of the optimization; Section 4 describes the different operation strategies in detail; Section 5 has a brief introduction about Genetic Algorithm; Section 6 presents results and carries out discussion; Section 7 draws the conclusions.

2 System and Components

2.1 System Schematic Layout

The system schematic layout is shown in Fig. 1, PV panels and storage (battery storage or hydrogen storage) are connected to the DC bus via DC-DC converters (controller). Grid and building load are connected to the 230 V AC bus. A bi-directional inverter locates between the AC and DC buses. The inverter and converters efficiency are all assumed as 0.95. The PV capacity is assumed as 200 kW$_p$, which is restricted by the available installation area. The system model is built partly based on OptiCE [24, 25]. The study is carried out with Matlab ® 2015b environment.

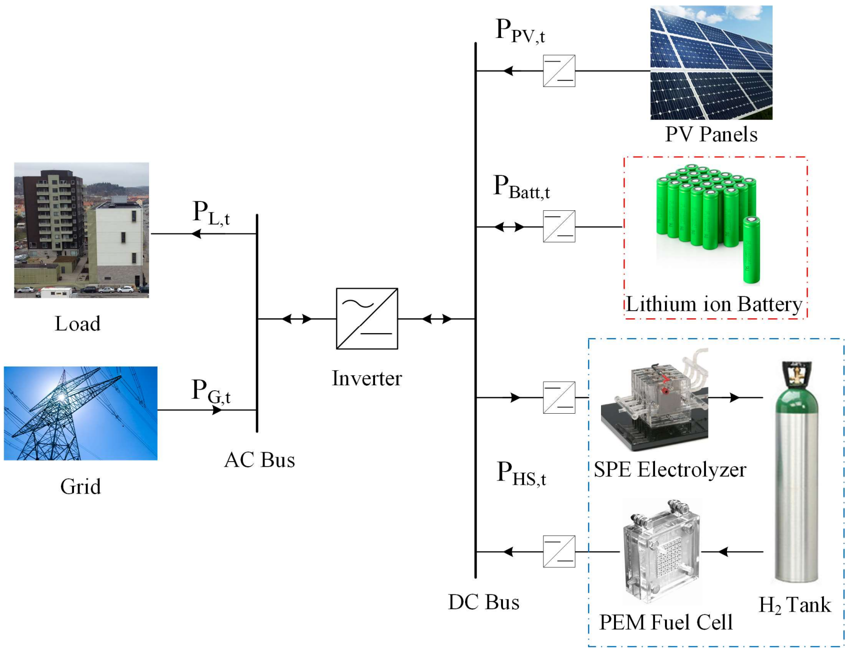

Fig. 1. System schematic layout

2.2 Single Diode Photovoltaic Model

The Voltage-Current ($V_{PV} - I_{PV}$) curve of the PV module is obtained with the single diode model [26] by Eq. (1):

$$I_{PV} = I_{PH} - I_0 \left[exp\left(\frac{V_{PV}+I_{PV} \cdot R_s}{a}\right) - 1 \right] - \frac{V_{PV}+I_{PV} \cdot R_s}{R_{sh}} \tag{1}$$

where, I_{PH} is the photocurrent (A); I_o is the diode reverse saturation current (A); a is the ideality factor (V); R_{sh} is the shunt resistance (Ω); R_s is the series resistance (Ω). I_{PH}, I_o, a, R_{sh} are variables subject to weather input and installation conditions. They are calculated with the method in Duffie and Beckman [27] and De Soto et al.[26].

The PV panels are connected to Maximum Power Point Tracking (MPPT) controllers. There are different MPPT algorithms, such as fuzzy logic control and the P&O method [16, 28]. In this study, the MPPT controller is simulated with simplified approach given in Eq. (2).

$$P_{PV,mpp} = \max(I_{PV} \cdot V_{PV}) \tag{2}$$

The selected PV module is SUNTECH STP255-20/Wd. The characterizing parameters are taken from System Advisory Model [29] and can be found in Zhang et al. [11]. The installation azimuth angle and tilt angle are optimized as 0° and 36°, which ensure maximal yearly production.

2.3 Hydrogen Storage Model

The hydrogen storage system consists of three major components: electrolyzer, hydrogen tank and fuel cell. The electrolyzer converts electrical energy into chemical energy through the decomposition of water into hydrogen (H_2) and oxygen (O_2). The produced hydrogen is compressed and fed into the hydrogen tank for storage. The fuel cell carries out the reverse process of electrolysis and uses hydrogen (H_2) and oxygen (O_2)/air to generate electrical power. There are many types of electrolyzers and fuel cells, which are generally classified based on the electrolyte type. In this study, Solid Polymer Electrolyte (SPE) electrolyzer and Polymer Electrolyte Membrane (PEM) fuel cell are selected.

There are generally three modelling approaches for electrolyzer and fuel cell. The first approach assumes fixed efficiency [16, 21, 23, 30], which neglects the influence of working conditions. The second one employs the efficiency/voltage-current curves [18, 31]. It considers the influence of current on the voltage (activation loss, ohmic loss, etc.), while neglecting the influence of temperature and pressure. The third approach employs detailed dynamic model [19, 32], which further considers pressure and temperature. In this study, it is assumed that the temperature and pressure of electrolyzer and fuel cell stacks are regulated and remain constant [31]. Thus, the second approach is employed.

The Power-Current (P-I) curve of PEM fuel cell (POWERCELL S2) is obtained from the product brochure (Fig. 2) [33]. The SPE electrolyzer's Voltage-Current (V-I) curve is obtained from Li et al. [30]. It is assumed that the electrolyzer outlet hydrogen is further compressed from 0.6 MPa to 20 MPa. The compressor power (W_c) is calculated with the following equation:

$$W_c = C_p \frac{T_1}{\eta_c}\left(\left(\frac{P_2}{P_1}\right)^{\frac{r-1}{r}} - 1\right) m_{H_2} \quad (3)$$

where, C_p is the specific heat of hydrogen; T_1 is the inlet hydrogen temperature (293 K); P_1 and P_2 are the inlet and output pressures; r is the isentropic exponent of hydrogen (1.4); m_{H_2} is the mass flow rate of hydrogen (kg/ s). η_c is the compressor efficiency, which is taken as 0.7 [30].

The relationship between current (I, A) and hydrogen flow rate (m_{H_2}, kg/s) is given by Eq. (4):

$$m_{H_2} = \frac{2I \times \mu_F}{F} \quad (4)$$

where, μ_F is the current efficiency, which is usually very high (>99%) and assumed as 1 in this study. F is the Faraday constant (96485 C/mol).

At specific current, the compressor power can be obtained through Eqs. (3) and (4). The overall Power-Current curve of electrolyzer and compressor is shown in Fig. 2

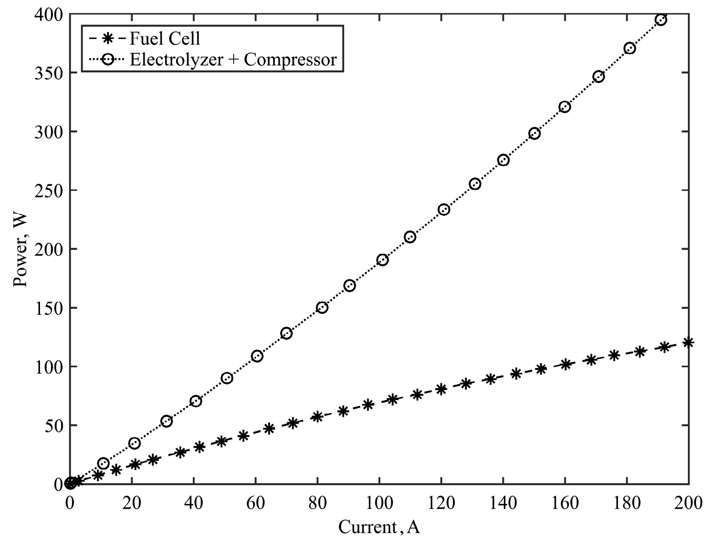

Fig. 2. Power-Current curves of fuel cell and combined electrolyzer and compressor

The state of hydrogen level ($SOH2_t$) is defined as the ratio of the stored hydrogen mass to the tank capacity.

$$SOH2_t = M_t / CAP_{HT} \quad (5)$$

The stored hydrogen mass M_t is calculated by Eq. (6):

$$M_t = M_{t-1} + \int m_{H_2} dt \quad (6)$$

Fixed lifetimes are assumed for the components of the hydrogen storage system.

2.4 Battery Model

Lithium ion batteries outperform other types of batteries in many aspects [34] and their costs have dropped substantially in recent years [34-36]. Lithium ion battery is chosen as the type of battery storage in this study.

The battery voltage-current relationship is represented by the Improved Shepherd model, which is developed by Tremblay et al. [37, 38]. The model describes the charging and discharging curves with Eqs. (7) and (8), respectively:

$$V = E_0 - K \frac{Q}{0.1Q + \int it} \cdot i^* - K \frac{Q}{Q - \int it} \int it + A \cdot e^{-B \cdot \int it} - i \cdot R \qquad (7)$$

$$V = E_0 - K \frac{Q}{Q - \int it} \cdot i^* - K \frac{Q}{Q - \int it} \int it + A \cdot e^{-B \cdot \int it} - i \cdot R \qquad (8)$$

where, V is the battery voltage (V); i is the battery current (charge as negative); i^* is the filtered current. E_0 (battery open circuit voltage, V), K (polarization constant, V/(Ah) and polarization resistance, Ω), Q (battery capacity, Ah), A (exponential zone amplitude, V), R (the internal resistance, Ω), and B (the exponential zone time constant inverse, $(Ah)^{-1}$) are battery parameters taken from Tremblay et al. [37] and can be found in Zhang et al. [11].

The battery lifetime is firstly determined by the method used in Zhang et al. [11]. However, when the battery storage follows the hybrid operation strategy (Section 4.4), as the hybrid operation strategy decreases the yearly cycle numbers, the lifetime is always determined as 15 years, which is constrained by the battery calendar life (Eq. 7 in Ref. [11]). Fixed lifetime for the battery storage is then employed in this study.

2.5 Load and Weather Profile

2.5.1 Load Profile

A rental multi-apartment building in Gothenburg (N 57.70°, W 11.98°) is chosen as the case study. The building uses heat pump for space heating during the winter. The hourly electricity consumption is recorded from the building owner, Wallenstam AB.

2.5.2 Weather Profile

The local weather data, including global horizontal radiation (W/m^2), diffuse horizontal radiation (W/m^2), wind speed (m/s) and ambient temperature (°C), is obtained from Meteonorm [39].

The PV production profile is obtained from the PV model with weather profile as input. The system net power $P_{Net,t}$ is defined by Eq. (9). Its profile and histogram are shown in Fig. 3.

$$P_{Net,t} = P_{L,t} - P_{PV,t} \cdot \eta_{inv} \tag{9}$$

There is power shortage during the cold months and surplus electricity during the warm months [40]. This seasonal mismatch problem should be well addressed to improve the system performance.

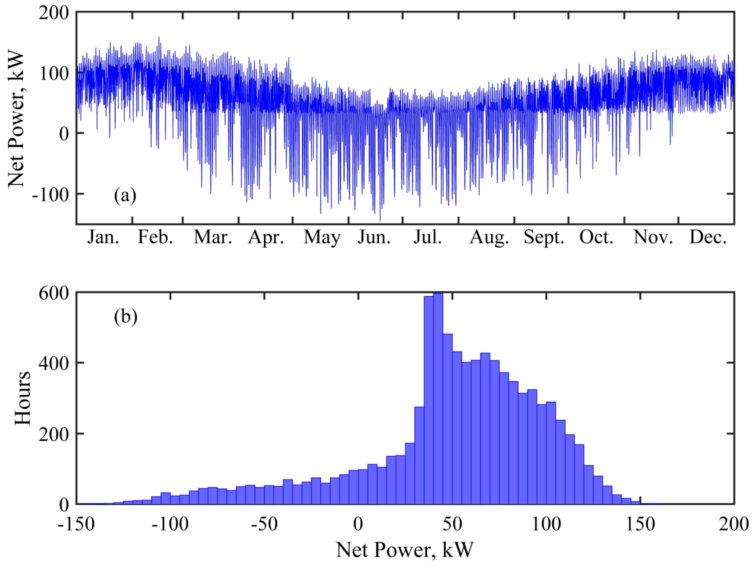

Fig. 3. (a) Hourly profile and (b) histogram of the net power (negative as exporting electricity to grid)

3 Optimization Objectives

For the end-users or prosumers, both economic and environmental goals are important. Net Present Value (NPV) and Self Sufficiency Ratio (SSR) are employed to represent these interests. The utility grid requires stable operation. They have interest in the impact of power flow between prosumers and grid. Grid Indicator (GI) is introduced to quantify the impact.

3.1 Net Present Value

3.1.1 System Revenue

The PV system owner buys electricity from the grid as retail electricity price ($El_{r,t}$) and sells electricity to the grid as the wholesale electricity price ($El_{w,t}$). Two variable components (Electricity Spot Price and Grid Fee) and one fixed component (Fixed Fee) make up the retail electricity price. The wholesale electricity price is the Electricity Spot Price (Elspot price), which is the day ahead hourly price from the electricity market Nord

Pool [41]. The Grid Fee comes from the contract with local utility grid, and it depends on the maximal power within the calendar year. The Fixed Fee includes energy tax, fixed grid charge, VAT, etc. In this study, grid fee and fixed fee are 0.83 SEK/kWh in total based on the current contract. It is consistent with the study by Sommerfeldt et al. [42]. When the yearly peak power is reduced, the economic benefit from grid fee reduction is assumed to be 1500 SEK/kW·Year, which is also obtained from the current contract with the local utility grid.

The system revenue is composed of three parts:

$$R_y = R_{ER,y} + R_{EX,y} + R_{PS,y} \tag{10}$$

where, $R_{ER,y}$ $R_{EX,y}$ and $R_{PS,y}$ are the electricity reduction revenue, export revenue and peak shaving revenue, respectively. They are calculated with Eqs. (11-16).

$$R_{ER,y} = \sum_{t=1}^{8760} \left(P_{L,t} - P_{Gim,t}\right) \cdot El_{r,t} \tag{11}$$

$$R_{EX,y} = \sum_{t=1}^{8760} P_{Gex,t} \cdot El_{w,t} \tag{12}$$

$$P_{PR} = max\left(P_{L,t}\right) - max\left(P_{Gim,t}\right) \tag{13}$$

$$R_{PS,y} = P_{PR} \times 1500 \tag{14}$$

$$P_{Gex,t} = \begin{cases} \left|P_{G,t}\right|, P_{G,t} \leq 0 \\ 0, P_{G,t} > 0 \end{cases} \tag{15}$$

$$P_{Gim,t} = \begin{cases} P_{G,t}, P_{G,t} > 0 \\ 0, P_{G,t} \leq 0 \end{cases} \tag{16}$$

$P_{L,t}$ is the load at time t; $P_{Gim,t}$ and $P_{Gex,t}$ are imported and exported grid power at time t. P_{PR} is grid peak power reduction (kW).

3.1.2 System Cost

In this study, the battery system price refers to the Tesla Powerwall [43], which includes battery pack and controller. The PV system turnkey cost, including inverter, installation and balance-of-plant cost, is obtained from the 2014 Swedish PV market report [44]. The cost information is summarized in Table 1.

Table 1. Unit investment cost, lifetime and Operation and Maintenance (O&M) ratio of battery and PV.

Module	Unit Investment Cost (UIC_i)	Lifetime	O&M Ratio ($r_{O\&M,i}$)
Lithium ion Battery System	3966 SEK/kWh	15 Years	0.5%/Year
PV system	12900 SEK/kW$_p$	25 Years	1%/Year

Literature review about the hydrogen storage components' cost is summarized in Table 2. Though the unit costs differ in the references, electrolyzer and fuel cell unit cost are all higher than 1000 $/kW. However, some optimistic cost estimations are also reported. Both the U.S. Department of Energy (DOE) [45] and the National Renewable Energy Laboratory (NREL) [46] estimated the electrolyzer production cost as 384 $/kW, and predicted future cost as 171 $/kW . DOE carried out a cost analysis for the fuel cell system and reported the system cost as low as 216 $/kW with yearly production of 1000 units. When the yearly production units increased to 10000 and 500000 pieces, the system cost can be further lowered to 103 and 40 $/kW [47]. Guerrero Moreno et al. had similar conclusions in a review paper [48].

Table 2. Literature review about hydrogen storage system cost

Reference	Year	Electrolyzer	Electrolyzer Lifetime	Hydrogen Tank	Hydrogen Tank Lifetime	Fuel cell	Fuel cell Lifetime
Li et al.[30]	2009	1000 $/kW	10 Y	30 $/kWh	20 Y	2500 $/kW	5 Y
Avril et al.[21]	2010	2535 $/kW	20 Y	1298 $/ kg	10 Y	3350 $/kW	20000 H
Türkay et al. [49]	2011	3128 $/kW	~	715 $/kWh	~	5000 $/kW	~
Castaneda et al. [18]	2013	7946 $/kW	30000 H	4646 $/kg	20 Y	5833 $/kW	30000 H
Safari et al [32]	2013	2000 $/kW	~	30 $/kWh	~	3000 $/kW	~
Silva et al.[50]	2013	17000 $/kW	15 Y	~	25 Y	8400 $/kW	30000 H
Zakeri et al.[51]	2014	1563 $/kW	~	~	~	3621 $/kW	~
Guinot et al. [52]	2015	3797 $/kW	5000 H	670 $/kg	25 Y	3015 $/kW	26200 H
Kalinci et al. [53]	2015	5000 $/kW	15 Y	577 $/kg	20 Y	4080 $/kW	30000 H

Y: Year. H: Working hours.

In this study, two cost scenarios are employed. The cost assumption in Kalinci et al [53] is taken as the pessimistic cost scenario. The exchange rate from USD to SEK is 8.46, corresponding to 42300 SEK/kW, 4881 SEK/kg and 34517 SEK/kW for electrolyzer, hydrogen tank and fuel cell, respectively. With the optimistic cost scenario, it is assumed that the unit cost for electrolyzer and fuel cell drops 90% and hydrogen tank unit cost drops 50%. In all, the pessimistic cost scenario is in line with the researches in Table 2, and the optimistic cost scenario is in line with the reports of DOE and NREL. It should be noted that the optimistic cost scenario is likely achievable, considering the fuel cell car Toyota Mirai, which has a 114 kW fuel cell stack, is sold with price of 57,500 $ without any subsidies.

The lifetime for electrolyzer, hydrogen tank and fuel cell are assumed as 15 years, 20 years and 30000 working hours, which also come from Kalinci et al [53]. The O&M Ratio for electrolyzer, fuel cell and hydrogen tank are all assumed as 1%/Year.

The system investment cost is obtained with Eq. (17):

$$Inv = \sum_{i=1}^{n} UIC_i \cdot CAP_i \tag{17}$$

where, UIC_i is the Unit Investment Cost for component i, and CAP_i is the capacity of component i.

The replacement cost ($C_{R,y}$) is assumed same as the investment cost. The operation and maintenance cost ($C_{O\&M,y}$) is calculated as:

$$C_{O\&M,y} = \sum_{i=1}^{n} UIC_i \cdot CAP_i \cdot r_{O\&M,i} \tag{18}$$

where, $r_{O\&M,i}$ is the O&M Ratio for component i.

NPV takes into account the system costs and revenues within the system life time (25 years). The discount rate (d_r) is chosen as 2%, considering current loan rate [54] and interest deduction for PV-related systems in Sweden [44].

$$NPV = \sum_{y=1}^{25} \frac{(R_y - C_{O\&M,y} - C_{R,y})}{(1+d_r)^{y-1}} - Inv \tag{19}$$

3.2 Self Sufficiency Ratio

SSR is defined with Eq. (20) [4]. It represents the percentage of the load that is met by the system, indicating the renewable energy penetration level.

$$SSR = \left(1 - \frac{\sum_{1}^{8760} P_{Gim,t}}{\sum_{1}^{8760} P_{L,t}}\right) \cdot 100\% \tag{20}$$

SSR can reflect the value of on-site renewable energy penetration from the perspective of building owner. It is calculated based on the on-site load and generation profiles and has been used in many studies [20, 40, 55, 56].

3.3 Grid Indicator

Current studies use different indicators to quantify the impact of power flow between prosumers and grid. Some focus on the maximal feed-in power [56-59]. Some studies emphasize the power fluctuation, employing the standard deviation of power as indicator [60, 61]. There are also studies stress the time-response of the grid, using ramp rate as indicator [55, 56]. In this study a dimensionless factor is introduced, which includes the dimensionless ratios of the above indicators.

The indicator, namely "Grid Indicator (GI)", is shown in Eq. (21). The case without storage is used as the reference. When there is storage, the standard deviation of exported power (P_{Gex}), the mean ramp rate of exported power (P_{Gex}) and maximal fee-in power are calculated and divided by the reference value. The sum of three dimensionless values are defined as Grid Indicator (GI). This value can represent the quality of the export electricity.

Smaller value represents that the system has less negative impact on grid. It is used as an optimization objective in Section 6.2.3.

$$GI = \frac{(STD(P_{Gex}))_{PV+Storage}}{(STD(P_{Gex}))_{Only\ PV}} + \frac{\left(MEAN(|P_{Gex,t+1} - P_{Gex,t}|)\right)_{PV+Storag}}{\left(MEAN(|P_{Gex,t+1} - P_{Ge\ \ ,t}|)\right)_{Only\ PV}} + \frac{(MAX(P_{Gex}))_{PV+Storage}}{(MAX(P_{Gex}))_{Only\ PV}} \quad (21)$$

4 Operation Strategies

In this section, three rule-based operation strategies for hydrogen storage and one rule-based operation strategy for battery storage are described. Within each operation strategy (except the conventional operation strategy), there are several operation conditions. Each operation condition is represented by one linear programming problem with specific objective and constraints. Some operation parameters are introduced to assign each time interval (t) with specific operation condition. The system power flow is determined by solving the linear programming problem at each time interval.

4.1 Conventional Operation Strategy

Conventional Operation Strategy refers to the most commonly used operation strategy of the energy storage system. The surplus of electricity from the PV system will be firstly stored and then exported to grid if the storage system is full. The insufficient electricity will be firstly provided by storage and then by grid. The hydro-gen storage acts as the buffer between generation and consumption. This strategy is also called “Maximizing Self-Consumption Strategy” [59]. This operation strategy has one operation condition, which is summarized as a linear programming problem (Fig. 4). Detailed explanation can be found in Ref. [11].

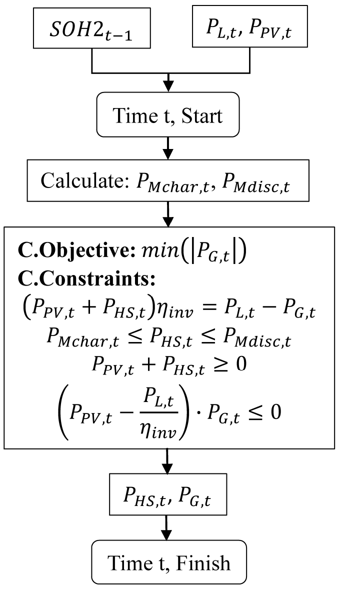

Fig. 4. Flowchart of the conventional operation strategy

4.2 Peak Shaving Strategy

Hydrogen storage is suitable for seasonal storage. If the stored hydrogen from warm months is used for peak shaving during the cold months, both $R_{ER,y}$ and $R_{PS,y}$ are increased, representing a cost-efficient way to use the store hydrogen. One system parameter (grid peak limit, P_{PL}) is introduced. The operation strategy is summarized in Fig. 5.

If the net power $P_{Net,t}$ is lower than P_{PL}, the storage will be charged when applicable. Constraint $P_{Mchar,t} \leq P_{HS,t} \leq 0$ suggests that the storage only charges.

When $P_{Net,t}$ is higher than P_{PL}, the storage will be discharged. The strategy maintains the grid power as P_{PL} (objective: $min(P_{G,t})$ and constraint: $P_{G,t} \geq P_{PL}$) if possible. The stored hydrogen is preserved only for peak shaving.

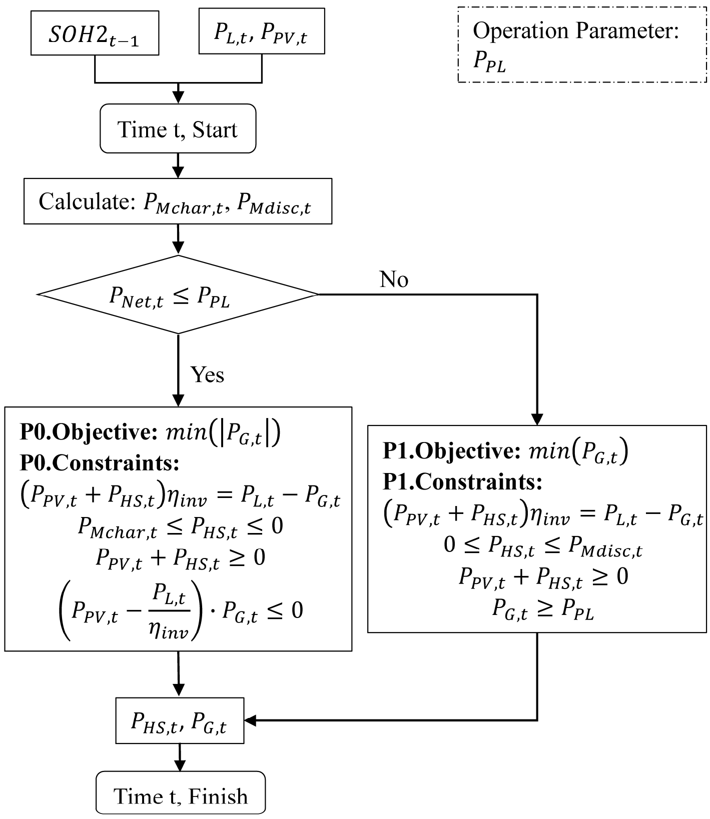

Fig. 5. Flowchart of the peak shaving strategy

4.3 Hybrid Operation Strategy

The hybrid operation strategy combines the conventional operation strategy and peak shaving strategy. Four operation parameters (P_{PL}, $SOH2_L$, t_s and t_e) are introduced. The strategy is summarized in Fig. 6. During the warm months ($t_s \leq t \leq t_e$), the operation condition is further determined by the hydrogen level. If $SOH2_{t-1}$ is higher than the hydrogen level limit $SOH2_L$, the system follows HH0, which is the conventional operation strategy. If $SOH2_{t-1}$ is lower than $SOH2_L$, the system will follow HH1, which charges the hydrogen storage but not discharge. During cold months ($t \leq t_s \vee t \geq t_e$), the operation strategy follows the peak shaving strategy, which is represented by two operation conditions (HH1, HH2). The operation conditions (HH1, HH2) are the same with those in Section 4.2 (P0, P1).

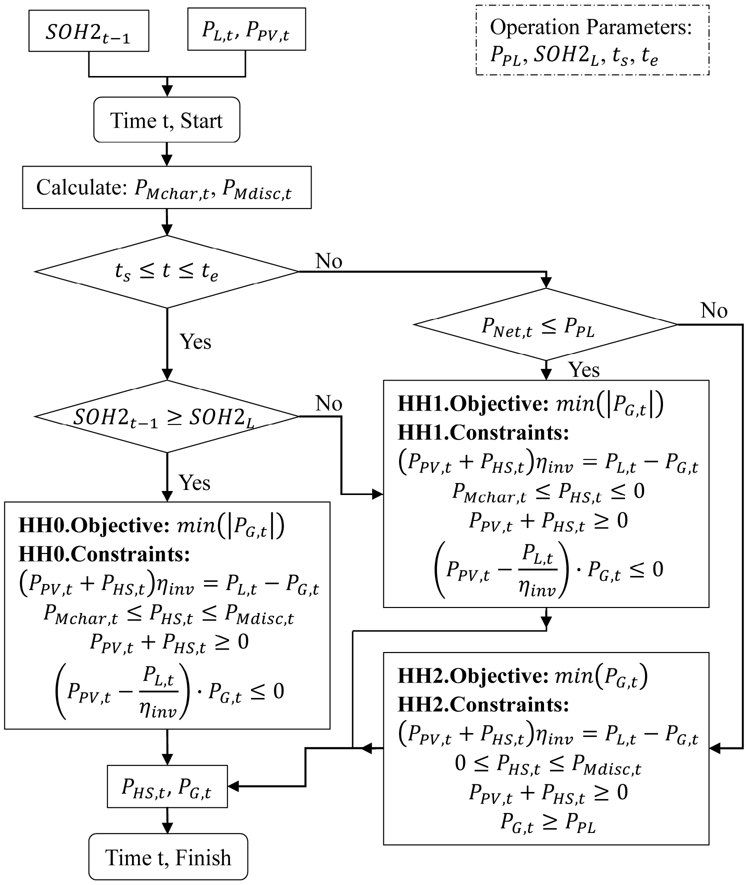

Fig. 6. Flowchart of the hybrid operation strategy

4.4 Hybrid Operation Strategy of Battery Storage

The battery hybrid operation strategy is firstly introduced in Ref. [11]. It is briefly explained to facility the smooth reading (Fig. 7). Four operation parameters (P_{PL}, P_{CL}, t_s and t_e) are introduced. During warm months ($t_s \leq t \leq t_e$), the system follows the conventional operation strategy (BH0). During cold months ($t \leq t_s \vee t \geq t_e$), the system is further represented by three operation conditions. If $P_{Net,t}$ is higher than P_{PL} (BH1), the battery is discharged to carry out peak shaving. If $P_{Net,t}$ is between P_{PL} and P_{CL}, the battery power is zero to maintain current SOC (BH2). If $P_{Net,t}$ is lower than charge limit P_{CL}, battery is charged from either PV or grid (BH3), during which the power balance of the system depends on the power flow of the system, indicating that the grid power can be used to charge the battery ($P_{PV,t} + P_{Batt,t} < 0$).

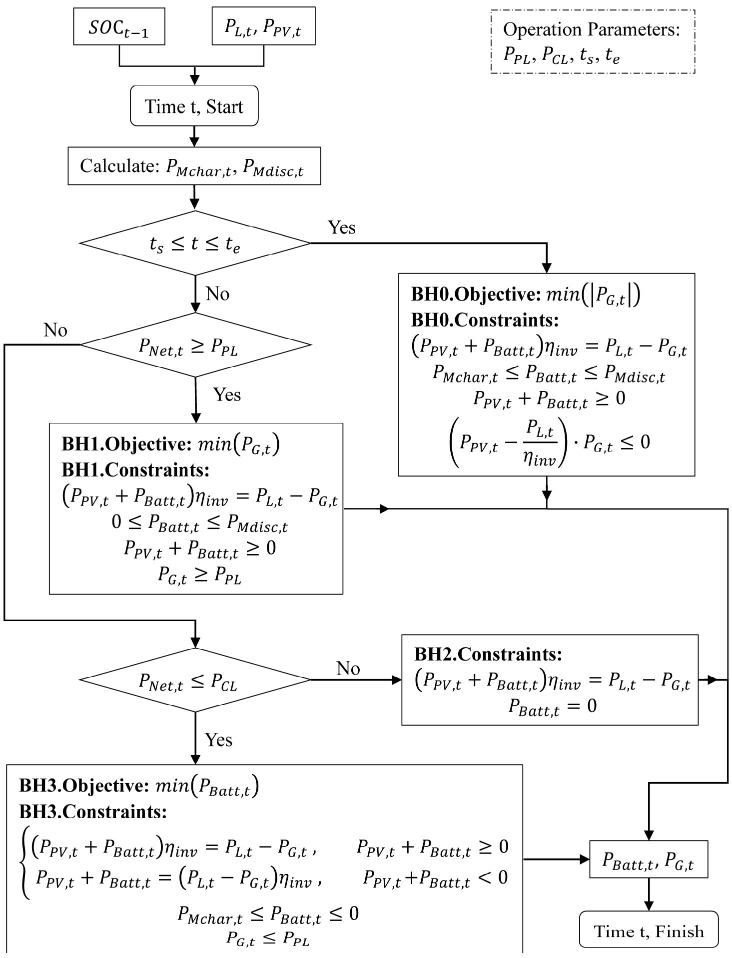

Fig. 7. Flowchart of the battery hybrid operation strategy

Hydrogen storage cannot fit into the operation strategies for battery storage, which are studied in [11]. The peak shaving strategy and hybrid operation strategy are introduced and tailored to take advantage of the hydrogen storage characteristics. The hydrogen storage has low round trip efficiency and long storage period, the seasonal stored hydrogen is only used to fulfill the peak loads, which help to gain higher revenue than fulfilling ordinary load. This is the major difference with the battery hybrid operation strategy, which charges from grid to fulfill the peak load

These operation strategies are designed based on the analysis of the representative case in Nordic countries. It should be noted that there might be other operation strategies that include feed-in-tariff, ancillary service provision, market arbitrage, least storage degradation, etc. However, feed-in tariff and ancillary services are not covered in the Swedish prosumers' contract now. Market arbitrage strategy has been studied in our previous paper [11], the result shows that it is unprofitable because the electricity price variation is not significant enough. The least storage degradation strategy relies on concrete electrochemical models, which are beyond the content of this manuscript. Within the employed approach, more sophisticated rule-based operation strategies for different cases can be further investigated.

5 Genetic Algorithm

Genetic Algorithm (GA), as a well-suited meta-heuristic tool [5, 62], is employed in this study to carry out multi-objective optimization. The objectives are NPV, SSR and GI (Only in Section 6.2.3). The variables are the component capacities and system operation parameters (Section 3 and 4). The optimization results are presented in the form of near-optimal Pareto front, which is a set of individuals that are non-dominated with respect to each other [63]. During the optimization, the upper bound for electrolyzer, fuel cell and hydrogen tank capacities are 100 kW, 100 kW and 300 kg.

The overall flowchart of the optimization is shown in Fig. 8. The detailed GA configuration parameters can be found in Zhang et al. [11].

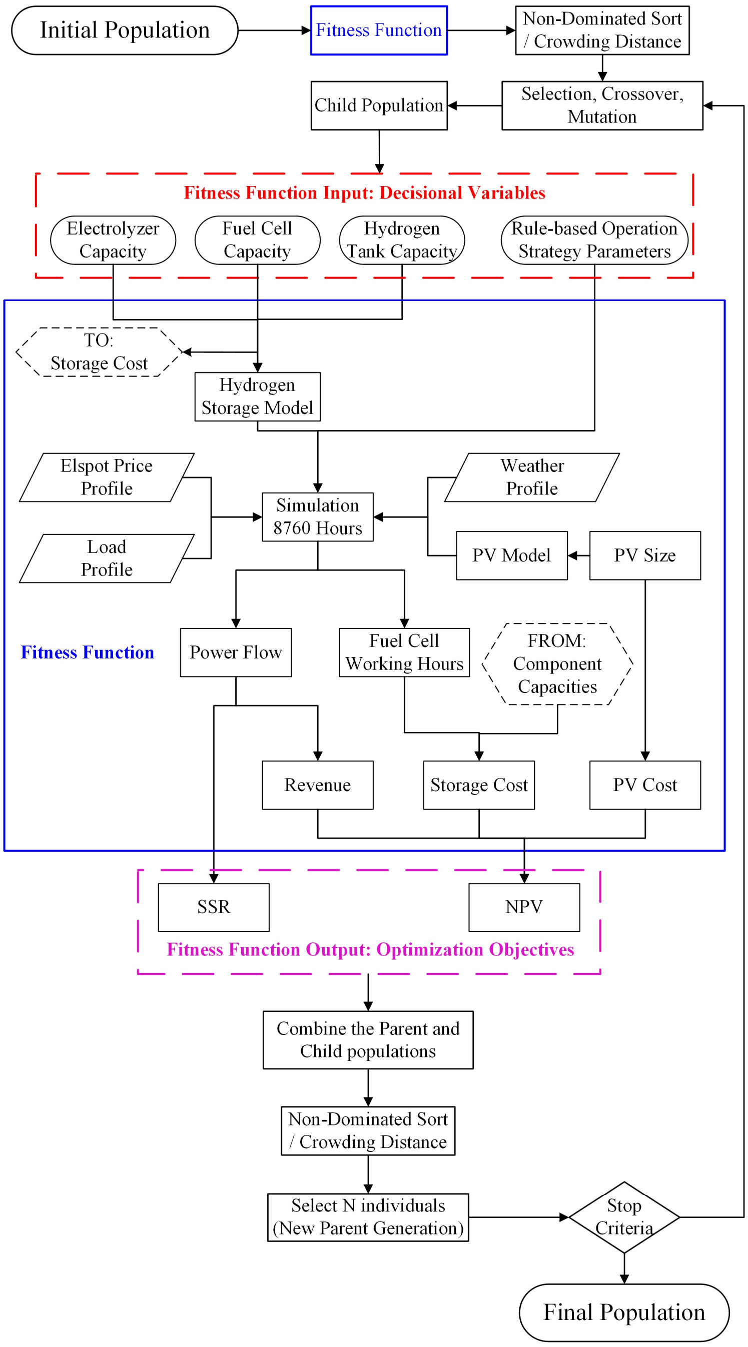

Fig. 8. Flowchart of the optimization process

6 Results and Discussion

The near-optimal Pareto fronts of different operation strategies are compared under either the pessimistic or the optimistic cost scenario (Cost scenarios are described in Section 3.1.2). The results are analyzed in Sections 6.1 and 6.2, respectively. The near-optimal Pareto front individuals' component capacities under the optimistic cost scenario are further analyzed in section 6.3.

6.1 Pessimistic Cost Scenario

The near-optimal Pareto fronts of different operation strategies under the pessimistic cost scenario are shown in Fig. 9. For the hydrogen storage, the hybrid operation strategy and the conventional operation strategy are superior to the peak shaving strategy that they achieve higher SSR at the same NPV. All the three operation strategies achieve the highest NPV when without hydrogen storage. It indicates that hydrogen storage cannot bring economic benefits for users under the pessimistic cost scenario. The near-optimal Pareto front of battery hybrid operation strategy is also shown in Fig. 9. Compared with hydrogen storage, battery storage achieves higher SSR at the same NPV. Moreover, some individuals achieve higher NPV than the system without storage, bringing in economic incentive for the PV-system user.

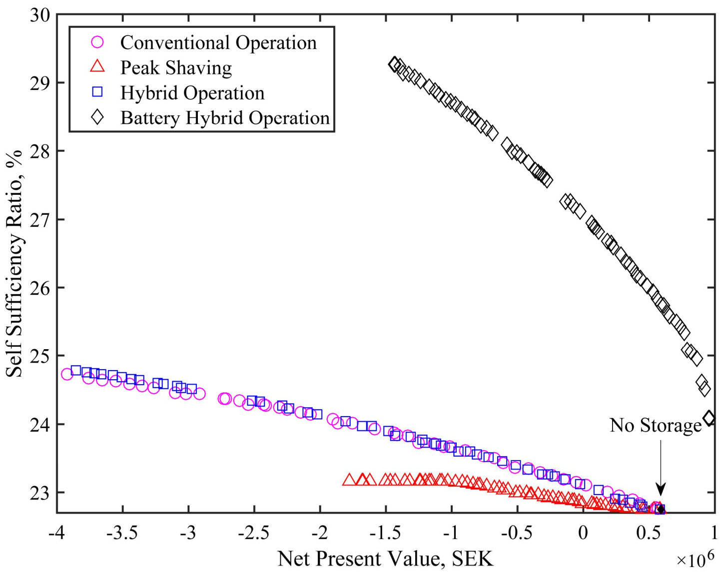

Fig. 9. Near-optimal Pareto fronts of different operation strategies under the pessimistic cost scenario

6.2 Optimistic Cost Scenario

The near-optimal Pareto fronts of different operation strategies under the optimistic cost scenario are shown in Fig. 10. During the optimization, NPV is constrained to be positive.

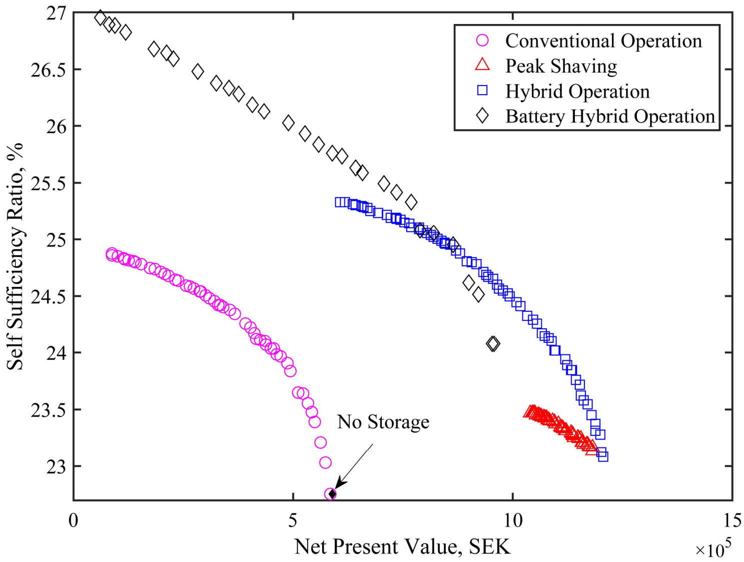

Fig. 10. Near-optimal Pareto fronts of different operation strategies under the optimistic cost scenario

The near-optimal Pareto fronts of different operation strategies change substantially compared with those under the pessimistic cost scenario. All the near-optimal Pareto fronts move towards higher NPV. But the highest NPV that each operation strategy achieve are different. With the conventional operation strategy, the highest NPV is achieved by the individual without storage. It suggests that the conventional operation strategy cannot bring in economic benefits even under the optimistic cost scenario. It addresses the importance of appropriate operation strategies, which can utilize the energy storage more efficiently. Compared with the system without storage, the individuals from the peak shaving strategy and the hybrid operation strategy achieve higher NPV and SSR concurrently.

The conventional operation strategy can achieve higher SSR than peak shaving strategy because it carries out more charge and discharge cycles; while the peak shaving strategy has higher NPV because it harvests the economic benefits from the peak shaving. The hybrid operation strategy combines the two operation strategies and includes the advantages of both.

The near-optimal Pareto front of the battery hybrid operation strategy (part of the near-optimal Pareto front that is shown in Fig. 9) is shown in Fig. 10. It intersects with that of the hydrogen hybrid operation strategy. The highest NPV that it achieves is lower than that of the hydrogen hybrid operation strategy. The grid power ($P_{G,t}$) and storage level ($SOH2_t$ and SOC_t) profiles of two closing individuals, which come from the near-optimal Pareto fronts of the hydrogen hybrid operation strategy and the battery hybrid operation strategy respectively, are shown in Fig. 11. The individuals' component capacities, first year revenue, etc. are listed in Table 3. The two individuals both have daily cycles during the warm months and carry out peak shaving during the cold months. For peak shaving, the hydrogen individual mainly uses stored hydrogen, while the battery individual depends on the charging from the grid. The two individuals have similar $R_{ER,1}$ and $R_{PS,1}$. The difference in the revenue at year 1 (R_1) is mainly due to the difference in export revenue ($R_{EX,1}$). Because the battery individual regularly gets fully charged and loses the ability to store excess electricity, leading to higher exportation.

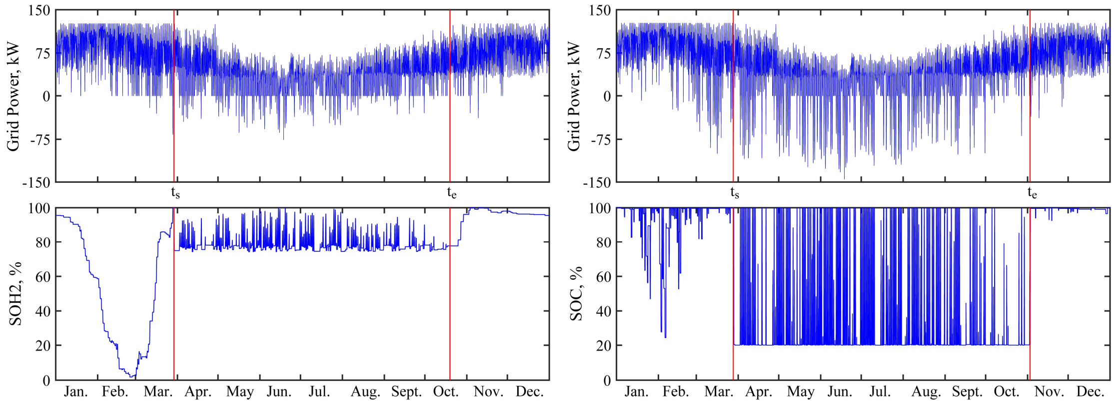

(a) (b)

Fig. 11. Grid power ($P_{G,t}$) and storage level profiles of (a) hydrogen storage and (b) battery storage individual

Table 3. Detailed information of the individual with hydrogen storage or battery storage

Category	Item	Hydrogen hybrid operation	Battery hybrid operation
Optimization Objectives	NPV (SEK)	820318	819198
	SSR (%)	25.0	25.1
Component Capacities	CAP_{EZ} (kW)	73	-
	CAP_{FC} (kW)	34	-
	CAP_{HT} (kg)	53	-
	CAP_{Batt} (kWh)	-	147
First Year Revenue	$R_{ER,1}$ (SEK)	183253	183624
	$R_{EX,1}$ (SEK)	2215	12029
	$R_{PS,1}$ (SEK)	48539	47280
	R_1 (SEK)	234007	242933
Grid Peak Power Reduction	P_{PR} (kW)	32.4	31.5

Under the optimistic cost scenario, the hydrogen storage achieves comparable performance as the battery storage. However, it should be noted that the studied case has strong seasonal mismatch between production and load, which favors hydrogen storage because it is advantageous in long period storage. Moreover, the comparable performance is achieved when the hydrogen storage system cost is under the optimistic cost scenario. However, the battery storage system's cost is based on current market price, and the battery industry is well boosted from the electric vehicle industry and a continuous price dropping is expected. Another disadvantage of the hydrogen storage is the system complexity (three components other than one, and having moving parts). Due to the above reasons, the battery storage system is suggested even when the hydrogen storage system is under the optimistic cost scenario.

6.2.1 Uncertainty Analysis with the Storage Lifetime

This study assumes fixed battery and hydrogen storage component lifetime. However, in real applications, the lifetime depends on many factors. The change in lifetime can influence system NPV. Uncertainty analysis by Monte Carlo simulation is carried out for the near-optimal Pareto fronts of hydrogen hybrid operation strategy and battery hybrid operation strategy (from Fig. 10). It is assumed that all the storage components' lifetime subject to uniform distribution with the variation limit of ±10%. The system simulations are repeated 4000 times with randomly generated component lifetimes.

The results are shown in Fig. 12. The error bars represent the lower and upper value at the desired level of confidence (95%), while the fixed point are the original values (in Fig. 10). The results indicate that with the decrease of NPV (which follows the increase of storage capacity), the influence of lifetime uncertainty on NPV enlarges. However, the variation of NPV is generally in limited range. This is mainly due to the studied grid-connected system employs relatively small storage capacity. Meanwhile, the uncertainty analysis indicates that the comparison results between battery and hydrogen storage is not challenged by the uncertainties in lifetime.

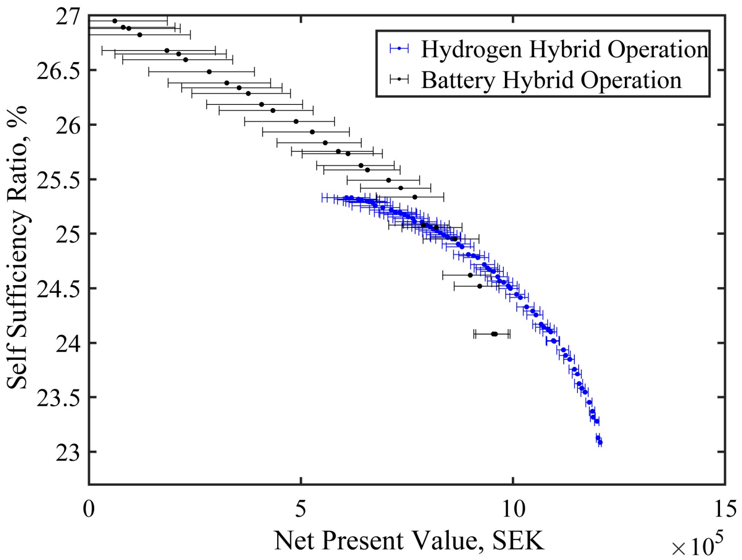

Fig. 12. Uncertainty analysis of the Pareto front individuals from Fig. 10.

6.2.2 Influence of Operation Strategies on the Component Capacities

The near-optimal Pareto front individuals' electrolyzer capacity, fuel cell capacity and hydrogen tank capacity against NPV are shown in Fig. 13. With the increase of the hydrogen storage capacity (all the components' capacities increase, or at least one component's capacity increases while others remain the same), NPV decreases under all the three operation strategies.

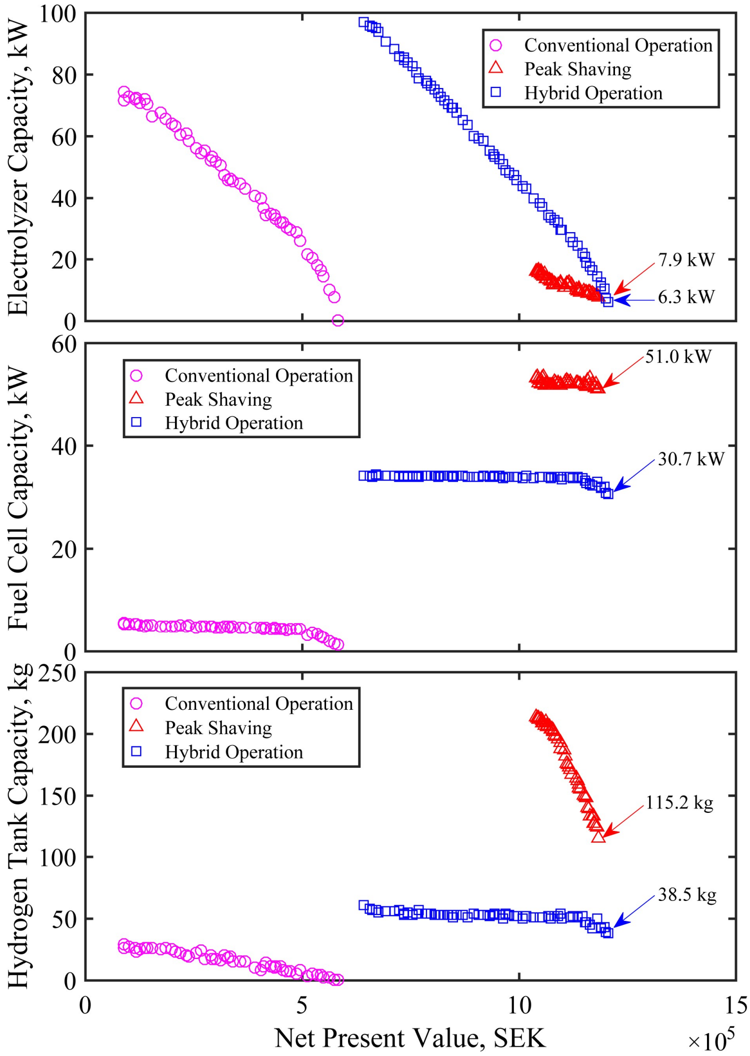

Fig. 13. Electrolyzer capacity, fuel cell capacity and hydrogen tank capacity of the near-optimal Pareto front individuals under the optimistic cost scenario (same individuals as in Fig. 10).

With the peak shaving strategy and hybrid operation strategy, the component capacities start to increase from specific values other than zero (shown in Fig. 13). The individuals with smaller storage capacities are missed from the near-optimal Pareto front. It is explained as those missing individuals achieve same NPV but lower SSR values than the individuals in near-optimal Pareto front. These individuals are excluded through the Elitism process.

The component capacities under different operation strategies have different changing patterns against NPV. It addresses the importance of concurrent optimization of component capacities and operation strategies.

6.2.3 Reducing System's Negative Impact on Grid

The growing distributed PV capacity can lead to operation problems in the grid [64]. In the above discussion, NPV and SSR represent the interest of end-users, while the system's impact on the grid is not included. Considering the potential restraints on exported electricity, the impacts of employing storage on the grid need to be considered when determining the storage type and storage capacity. It is necessary to understand the roles that different storage can play in reducing the system's negative impact on grid.

The battery storage under the current hybrid operation strategy (Fig. 7) cannot effectively control the exported electricity. During warm months the strategy maximizes the self-consumption (also increase SSR and Revenue) through charging the battery when there is excess PV production. Because of the relatively small battery capacity, it is fully charged before or shortly after noon. During the rest of daytime, the excess PV power is directly exported to the grid. The strategy can lead to high ramp rate, high feed-in power and high variation in export power.

The battery hybrid operation strategy is modified to smooth the power exportation (Fig. 14). During cold months, the operation strategy is same as that in Fig. 7. During warm months, a new operation parameter (P_E, negative value) is introduced. The battery is charged when $P_{Net,t}$ is lower than P_E (Operation Condition BH4). When $P_{Net,t}$ is higher than P_E, battery either maintains same SOC (BH2) or is discharged (BH5). The modified operation strategy only charges the battery when the exported electricity reaches certain level. The battery can maintain low SOC in the morning and helps to eliminate the export power peaks afterwards.

Within this approach, the trade-off between self-consumption and exportation control is coordinated by Genetic Algorithm through finding the optimal match between operation parameters and storage capacity.

The hydrogen storage operation strategy remains the same as in Fig. 6. Because hydrogen storage can reduce the excess electricity exportation effectively during warm months, as shown in Fig. 11, with the current hybrid operation strategy. The GA can adjust the component capacities to fulfill the third objective GI.

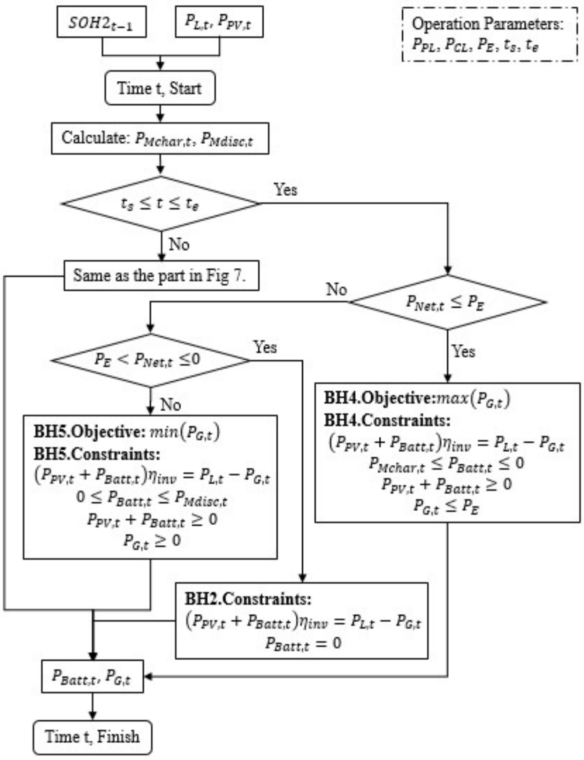

Fig. 14. Flowchart of the modified battery hybrid operation strategy

Even though it is still unclear which kind of restraint on PV exportation will be adopted by utility grid in the future, one common restraint is feed-in power limit, which has been applied in Germany [57, 59]. In this study, Feed-in limit of 50%, which is 100 kW, is applied.

The three objectives (SSR, NPV and GI) optimization are carried out by GA. The obtained Pareto fronts are shown in Fig. 15. For the battery storage, part of the Pareto front achieves higher NPV and SSR as well as lower GI compared with the no storage condition (black down-pointing triangle). It demonstrates the effectiveness of proposed operation strategy, which brings benefits not only to end-users but also utility grid. The highest NPV remains almost the same as the two objective optimization (Fig. 10). With the decrease of NPV, SSR slightly increase (as shown in the projection on SSR-NPV surface) and GI slightly decrease. However, the increase rate of SSR is much slower than that in Fig. 10. The battery's ability in increasing SSR is inhibited when fulfilling the GI objective.

For the hydrogen storage, SSR and GI also show the same trend with the decrease of NPV. However, the variation rates of SSR and GI are much higher than the battery storage. The projected curve on the SSR-NPV surface is almost the same as that obtained with two objectives optimization (Fig. 10). It indicates that hydrogen storage is more capable of smoothing the power flow without decreasing the other two objectives. Furthermore, hydrogen storage achieves higher SSR and lower GI than the battery storage at the same NPV. It indicates that hydrogen storage is a more favorable choice when considering the grid requirement.

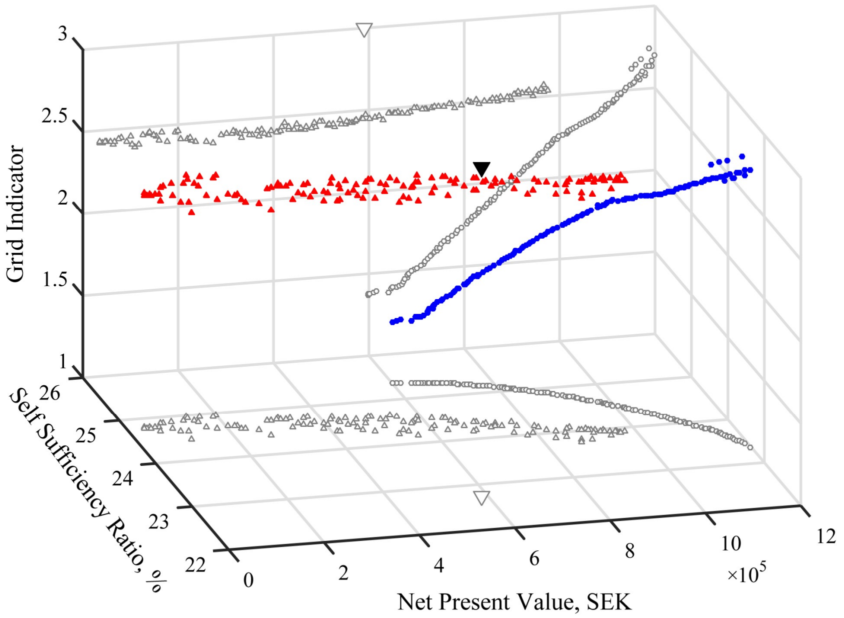

Fig. 15. Three objectives optimization and near-optimal Pareto fronts of PV-Battery/Hydrogen Storage systems (red triangle: Battery; blue circle: Hydrogen; black down-pointing triangle: No Storage; grey hollow markers: projections on the surface).

6.3 Discussions and Future Work

This study presents a ready-to-use tool for sizing grid-connected PV-hydrogen storage system. The comparison between the three operation strategies for the hydrogen storage system indicate that the pro-posed hybrid operation strategy achieves the best performance under both pessimistic and optimistic cost scenarios. The hybrid operation strategy should be recommended for similar cases in Nordic counties. It helps the system owner to achieve higher NPV and SSR. It is also beneficial to the grid in curtailing PV exportation during warm months and decreasing the peak demand during cold months. Moreover, it is applicable without the necessity of forecasting, which is usually not available for the small-scale end users. It is highly practical and provides direct guidance for real applications.

The study also provides building owners, building designers, grid-connected PV system owners and other stakeholders a decisional tool to choose the right type of storage. When considering only SSR and NPV, battery storage is recommended under both pessimistic and optimistic cost scenarios. However, hydrogen storage is recommended when taking GI into account under the optimistic cost scenario.

Future works need to be carried out with the following aspects. The proposed hybrid operation strategy applies to the studied case (or similar cases in Nordic countries), which has seasonal mismatch and locates in a deregulated electricity market. The applicability of this operation strategy to other cases should be tested. And other operation strategies, which include for instance, feed-in-tariff, ancillary service provision, market arbitrage, least storage degradation, should be designed and tested. Moreover, more accurate component models can be incorporated into the proposed framework. For example, the electrochemical components are assumed with fixed lifetime. Detailed and reliable lifetime models can be applied when available.

7 Conclusions

The following conclusions can be drawn:

1) Under the pessimistic cost scenario, the hybrid operation strategy and the conventional operation strategy are superior to the peak shaving strategy. Under the optimistic cost scenario, the peak shaving strategy and the hybrid operation strategy are superior to the conventional operation strategy.

2) The hybrid operation strategy includes the advantages of both the conventional operation strategy and the peak shaving strategy. It achieves the best performance among the three operation strategies under both pessimistic and optimistic cost scenarios.

3) Under the pessimistic cost scenario, hydrogen storage has poorer performance than battery storage in terms of NPV and SSR. Under the optimistic cost scenario, hydrogen

storage and battery storage achieve comparable results in terms of NPV and SSR. However, when taking into account the grid power fluctuation, hydrogen storage achieves better performance in terms of NPV, SSR and GI.

4) The hydrogen storage component capacities show different changing patterns against NPV with different operation strategies.

Acknowledgements

This work has received funding from KKS Future Energy Profile, European Union's Horizon 2020 (No. 646529) and National High Technology Research and Development Program (863 program) of China (No. 2015AA050403). The authors thank Wallenstam AB with the building load profile. One of the authors, Yang Zhang, acknowledges the financial support from China Scholarship Council (CSC).

Reference

[1] IEA-PVPS. Snapshot of global PV markets. 2015 <http://www.iea-pvps.org/>.

[2] IEA-PVPS. Trends 2014 in Photovoltaic applications. 2014 <http://www.iea-pvps.org/>.

[3] Castillo-Cagigal M, Caamaño-Martín E, Matallanas E, Masa-Bote D, Gutiérrez A, Monasterio-Huelin F, et al. PV self-consumption optimization with storage and Active DSM for the residential sector. Sol Energy 2011; 85: 2338-48.

[4] Luthander R, Widén J, Nilsson D, Palm J. Photovoltaic self-consumption in buildings: A review. Appl Energy 2015; 142: 80-94.

[5] Yang H, Zhou W, Lou C. Optimal design and techno-economic analysis of a hybrid solar–wind power generation system. Appl Energy 2009; 86: 163-9.

[6] Paliwal P, Patidar NP, Nema RK. Determination of reliability constrained optimal resource mix for an autonomous hybrid power system using particle swarm optimization. Renew Energy 2014; 63: 194-204.

[7] Riffonneau Y, Bacha S, Barruel F, Ploix S. Optimal power flow management for grid connected PV systems with batteries. IEEE Trans Sustain Energy 2011; 2: 309-20.

[8] Lu B, Shahidehpour M. Short-term scheduling of battery in a grid-connected PV/battery system. IEEE Trans Power Syst 2005; 20: 1053-61.

[9] Ru Y, Jan K, Sonia M. Storage size determination for grid-connected Photovoltaic systems. IEEE Trans Sustain Energy 2013; 4: 68-81.

[10] Khalilpour R, Vassallo A. Planning and operation scheduling of PV-battery systems: A novel methodology. Renew Sust Energy Rev 2016; 53: 194-208.

[11] Zhang Y, Lundblad A, Campana PE, Benavente F, Yan J. Battery sizing and rule-based operation of grid-connected photovoltaic-battery system: A case study in Sweden. Energy Convers Manage 2017; 133: 249-63.

[12] Leadbetter J, Swan LG. Selection of battery technology to support grid-integrated renewable electricity. J Power Sources 2012; 216: 376-86.

[13] Agbossou K, Kolhe M, Hamelin J, Bose TK. Performance of a stand-alone renewable energy system based on energy storage as hydrogen. IEEE Trans Energy Convers 2004; 19: 633-40.

[14] Díaz-González F, Sumper A, Gomis-Bellmunt O, Villafáfila-Robles R. A review of energy storage technologies for wind power applications. Renew Sust Energy Rev 2012; 16: 2154-71.

[15] Wallenstam AB and Midroc, Storage of Energy. <http://www.powercell.se/wallenstam-project> [assessed

[16] Bigdeli N. Optimal management of hybrid PV/fuel cell/battery power system: A comparison of optimal hybrid approaches. Renew Sust Energy Rev 2015; 42: 377-93.

[17] Carapellucci R, Giordano L. Modeling and optimization of an energy generation island based on renewable technologies and hydrogen storage systems. Int J Hydrogen Energy 2012; 37: 2081-93.

[18] Castañeda M, Cano A, Jurado F, Sánchez H, Fernández LM. Sizing optimization, dynamic modeling and energy management strategies of a stand-alone PV/hydrogen/battery-based hybrid system. Int J Hydrogen Energy 2013; 38: 3830-45.

[19] Parra D, Walker GS, Gillott M. Modeling of PV generation, battery and hydrogen storage to investigate the benefits of energy storage for single dwelling. Sustain Cities Soc 2014; 10: 1-10.

[20] Marino C, Nucara A, Pietrafesa M, Pudano A. An energy self-sufficient public building using integrated renewable sources and hydrogen storage. Energy 2013; 57: 95-105.

[21] Avril S, Arnaud G, Florentin A, Vinard M. Multi-objective optimization of batteries and hydrogen storage technologies for remote photovoltaic systems. Energy 2010; 35: 5300-8.

[22] Pellow MA, Emmott CJM, Barnhart CJ, Benson SM. Hydrogen or batteries for grid storage? A net energy analysis. Energy Environ Sci 2015; 8: 1938-52.

[23] García-Triviño P, Llorens-Iborra F, García-Vázquez CA, Gil-Mena AJ, Fernández-Ramírez LM, Jurado F. Long-term optimization based on PSO of a grid-connected renewable energy/battery/hydrogen hybrid system. Int J Hydrogen Energy 2014; 39: 10805-16.
[24] OptiCE. <www.optice.net> [assessed 11.8.2016].
[25] Campana PE, Li H, Zhang J, Zhang R, Liu J, Yan J. Economic optimization of photovoltaic water pumping systems for irrigation. Energy Convers Manage 2015; 95: 32-41.
[26] De Soto W, Klein SA, Beckman WA. Improvement and validation of a model for photovoltaic array performance. Sol Energy 2006; 80: 78-88.
[27] Duffie JA, Beckman WA. Solar engineering of thermal processes. 4th ed. Wiley New York etc.2013.
[28] Salas V, Olías E, Barrado A, Lázaro A. Review of the maximum power point tracking algorithms for stand-alone photovoltaic systems. Sol Energ Mat Solar C 2006; 90: 1555-78.
[29] Blair N, Dobos AP, Freeman J, Neises T, Wagner M, Ferguson T, et al. System advisor model, sam 2014.1. 14: general description. 2014 <https://www.nrel.gov/publications>.
[30] Li C-H, Zhu X-J, Cao G-Y, Sui S, Hu M-R. Dynamic modeling and sizing optimization of stand-alone photovoltaic power systems using hybrid energy storage technology. Renew Energy 2009; 34: 815-26.
[31] Darras C, Sailler S, Thibault C, Muselli M, Poggi P, Hoguet JC, et al. Sizing of photovoltaic system coupled with hydrogen/oxygen storage based on the ORIENTE model. Int J Hydrogen Energy 2010; 35: 3322-32.
[32] Safari S, Ardehali MM, Sirizi MJ. Particle swarm optimization based fuzzy logic controller for autonomous green power energy system with hydrogen storage. Energy Convers Manage 2013; 65: 41-9.
[33] High efficiency with water as the only emission. <http://www.powercell.se/products/fuel-cell/> [assessed 3.15.2016].
[34] Dunn B, Kamath H, Tarascon J-M. Electrical energy storage for the grid: A battery of choices. Science 2011; 334: 928-35.
[35] Yang Z, Zhang J, Kintner-Meyer MCW, Lu X, Choi D, Lemmon JP, et al. Electrochemical energy storage for green grid. Chem Rev 2011; 111: 3577-613.
[36] Nykvist B, Nilsson M. Rapidly falling costs of battery packs for electric vehicles. Nat Clim Change 2015; 5: 329-32.
[37] Tremblay O, Dessaint L-A. Experimental validation of a battery dynamic model for EV applications. World Electric Vehicle Journal 2009; 3: 1-10.
[38] Tremblay O, Dessaint L-A, Dekkiche AI. A Generic Battery Model for the Dynamic Simulation of Hybrid Electric Vehicles. In: 2007 IEEE Vehicle Power and Propulsion Conference (VPPC); 2007. p. 284-9
[39] List of all Meteonorm features <http://www.meteonorm.com/> [assessed 15.3.2016].
[40] Zhang Y, Lundblad A, Campana PE, Yan J. Employing battery storage to increase photovoltaic self-sufficiency in a residential building of Sweden. Energy Proc 2016; 88: 455-61.
[41] Nord Pool Spot. <http://www.nordpoolspot.com/> [assessed 11.3.2016].
[42] Sommerfeldt N, Madani H. On the use of hourly pricing in techno-economic analyses for solar photovoltaic systems. Energy Convers Manage 2015; 102: 180-9.
[43] Tesla home battery. <https://www.tesla.com/powerwall> [assessed 11.8.2016].
[44] Lindahl J. National survey report of PV power applications in SWEDEN. 2015 <http://www.iea-pvps.org/>.
[45] Ainscough C, Peterson D, Miller E. DOE Hydrogen and Fuel Cells Program Record. 2014 <https://www.hydrogen.energy.gov/program_records.html>.
[46] Saur G, Ramsden T. Wind Electrolysis: Hydrogen Cost Optimization. 2011 <http://www.osti.gov/bridge>.
[47] Marcinkoski J, Spendelow J, Wilson A, Papageorgopoulos D. Fuel Cell System Cost. 2015 <https://www.hydrogen.energy.gov/program_records.html>.

[48] Guerrero Moreno N, Cisneros Molina M, Gervasio D, Pérez Robles JF. Approaches to polymer electrolyte membrane fuel cells (PEMFCs) and their cost. Renew Sust Energy Rev 2015; 52: 897-906.
[49] Türkay BE, Telli AY. Economic analysis of standalone and grid connected hybrid energy systems. Renew Energy 2011; 36: 1931-43.
[50] Silva SB, Severino MM, de Oliveira MAG. A stand-alone hybrid photovoltaic, fuel cell and battery system: A case study of Tocantins, Brazil. Renew Energy 2013; 57: 384-9.
[51] Zakeri B, Syri S. Electrical energy storage systems: A comparative life cycle cost analysis. Renew Sust Energy Rev 2015; 42: 569-96.
[52] Guinot B, Champel B, Montignac F, Lemaire E, Vannucci D, Sailler S, et al. Techno-economic study of a PV-hydrogen-battery hybrid system for off-grid power supply: Impact of performances' ageing on optimal system sizing and competitiveness. Int J Hydrogen Energy 2015; 40: 623-32.
[53] Kalinci Y, Hepbasli A, Dincer I. Techno-economic analysis of a stand-alone hybrid renewable energy system with hydrogen production and storage options. Int J Hydrogen Energy 2015; 40: 7652-64.
[54] Sweden interest rates. <http://sweden.deposits.org/> [assessed 16.5.2016].
[55] Balcombe P, Rigby D, Azapagic A. Energy self-sufficiency, grid demand variability and consumer costs: Integrating solar PV, Stirling engine CHP and battery storage. Appl Energy 2015; 155: 393-408.
[56] de Oliveira e Silva G, Hendrick P. Lead–acid batteries coupled with photovoltaics for increased electricity self-sufficiency in households. Appl Energy 2016; 178: 856-67.
[57] Li J, Danzer MA. Optimal charge control strategies for stationary photovoltaic battery systems. J Power Sources 2014; 258: 365-73.
[58] Luthander R, Widén J, Munkhammar J, Lingfors D. Self-consumption enhancement and peak shaving of residential photovoltaics using storage and curtailment. Energy 2016; 112: 221-31.
[59] Moshövel J, Kairies K-P, Magnor D, Leuthold M, Bost M, Gährs S, et al. Analysis of the maximal possible grid relief from PV-peak-power impacts by using storage systems for increased self-consumption. Appl Energy 2015; 137: 567-75.
[60] Xu L, Ruan X, Mao C, Zhang B, Luo Y. An improved optimal sizing method for wind-solar-battery hybrid power system. IEEE Trans Sustain Energy 2013; 4: 774-85.
[61] Purvins A, Papaioannou IT, Debarberis L. Application of battery-based storage systems in household-demand smoothening in electricity-distribution grids. Energy Convers Manage 2013; 65: 272-84.
[62] González A, Riba J-R, Rius A, Puig R. Optimal sizing of a hybrid grid-connected photovoltaic and wind power system. Appl Energy 2015; 154: 752-62.
[63] Konak A, Coit DW, Smith AE. Multi-objective optimization using genetic algorithms: A tutorial. Reliab Eng Syst Safe 2006; 91: 992-1007.
[64] Shivashankar S, Mekhilef S, Mokhlis H, Karimi M. Mitigating methods of power fluctuation of photovoltaic (PV) sources – A review. Renew Sust Energy Rev 2016; 59: 1170-84.